

**REMOTE SENSING ASSESSMENT OF LAND  
COVER/LAND USE CHANGES AND ITS  
RELATIONSHIP ON LAND SURFACE  
TEMPERATURE IN PENANG ISLAND**

**TAN KOK CHOOI**

**UNIVERSITI SAINS MALAYSIA**

**2010**

REMOTE SENSING ASSESSMENT OF LAND  
COVER/LAND USE CHANGES AND ITS  
RELATIONSHIP ON LAND SURFACE  
TEMPERATURE IN PENANG ISLAND

by

TAN KOK CHOOI

Thesis submitted in fulfillment of the requirements  
for the degree of  
Master of Science

MAY 2010

## ACKNOWLEDGEMENTS

First of all, I want to sincerely appreciate and acknowledge all the related parties or individuals, in order to advice and help me, to finish this research. The most important person I need to 100 % pay my respect and thanks, without any doubt are both of my supervisors, Dr. Lim Hwee San and Associate Professor Mohd. Zubir Mat Jafri. They always guide, support, and help me especially I am facing the problem throughout the project. Thank you very much for their encouragement, attention and patient to guide me and finally I can finish the project to fulfill the requirement for Masters' study. Furthermore, the motivation provided by them promoted my dedication to finish my project and not felt so easily give up solving all the challenges throughout the project.

In addition, I also want to appreciate both of my beloved parents. Their convince and encouragement become main factor for me to successful conduct and finish the project on time in Universiti Sains Malaysia. Although we are stay far away, however their love and support catalyzed me to courage me to further the Masters' study and finish the project.

Besides that, thank you very much for the staffs in School of Phycis, Universiti Sains Malaysia, especially for their help and cooperative, who participates in this project directly or indirectly from initial till the end of the project. Without their help and participation, I think my project cannot conducted smoothly and finish on time.

Finally, I felt so grateful and proud that because I have a lot of lab mates, who are also conducted their research at the same laboratory with me. I wish to thank for their valuable experience and like to share their knowledge with me throughout the project.

**TAN KOK CHOOI**  
**2009**

## TABLE OF CONTENTS

	PAGE
<b>ACKNOWLEDGEMENTS</b>	ii
<b>TABLE OF CONTENTS</b>	iv
<b>LIST OF TABLES</b>	vii
<b>LIST OF FIGURES</b>	ix
<b>LIST OF ABBREVIATIONS</b>	xiii
<b>ABSTRAK</b>	xv
<b>ABSTRACT</b>	xvii
<b>CHAPTER 1 – INTRODUCTION OF REMOTE SENSING TECHNIQUE</b>	1
1.1 Introduction	1
1.1.1 Landsat TM/ETM+	4
1.2 Urban Heat Island Effects (UHI)	7
1.3 History of Thermal Infrared for Urban Climate	9
1.4 Literature Review	10
1.5 Problem Statement	19
1.6 Objectives	21
1.7 Research Scope	22
1.8 Summary of the Thesis	23
<b>CHAPTER 2 – Methodology</b>	25
2.1 Introduction	25
2.2 Study Area	25
2.3 Remotely Sensed Data	27
2.4 Materials	28

2.4.1	Landsat Images	29
2.4.2	Digital Elevation Model	34
2.5	Image Pre-Processing	34
2.6	Image Processing	35
2.6.1	Radiometric Calibration	37
2.6.2	Relative Radiometric Normalization Technique	39
2.6.3	Image Classification	41
2.6.3.1	Supervised Classification	43
2.6.4	Land Surface Temperature (LST) Retrieval	45
2.6.5	NDVI Computation	46
2.6.6	Cloud Masking	47
2.6.7	Land Surface Emissivity Estimation from the NDVI Method	49
2.6.7.1	LST Retrieval from Emissivity Value Estimated By NDVI Method	50
2.6.8	Omission and Commission Error in Image Classification	52
2.7	Software	53
2.7.1	PCI Geomatica 10.1 Image Processing Software	53
2.8	Conclusion	54
	<b>CHAPTER 3 – DATA ANALYSIS AND RESULTS</b>	56
3.1	Introduction	56
3.2	Relative Radiometric Normalization Technique of Imagery	56
3.2.1	NDVI Computation Based on the Relative Radiometric Normalization Technique	62
3.3	Image Classification	69
3.3.1	LULC Changes and Analysis in Penang Island, From	86

1991-1997

3.4	Urbanization Impact on LST	93
3.5	Relationship between LST and NDVI	100
3.6	Discussion	113
3.7	Conclusion	119
	<b>CHAPTER 4 – VALIDATION OF THE TECHNIQUES</b>	120
4.1	Introduction	120
4.2	Validation of TOA Reflectance with the Surface Reflectance	120
4.3	Validation of Land Surface Temperature (LST)	127
4.4	Discussion	136
4.5	Conclusion	138
	<b>CHAPTER 5 – CONCLUSION AND FUTURE WORKS</b>	139
5.1	Introduction	139
5.2	Conclusion	139
5.3	Future Works	144
	<b>REFERENCES</b>	148
	<b>APPENDICES</b>	158
	<b>LIST OF PUBLICATIONS AND CONFERENCE PAPERS</b>	162

## LIST OF TABLES

	PAGE
1.1 Landsat spectral bands and the application in remotely sensed data.	6
2.1 Product description for Landsat images and the parameters need to be inputted for the module for ATCOR3_T.	29
2.2 Classification classes description of Landsat images.	43
3.1 Summary of the relative radiometric normalization acquired after regression analysis.	62
3.2 The overall classification accuracy and Kappa coefficient for the land cover map, 1991.	72
3.3 Error matrix of the LULC map, 1991.	73
3.4 The commission and omission errors for the land cover map, 1991.	74
3.5 The overall classification accuracy and Kappa coefficient for the land cover map, 1999.	76
3.6 Error matrix of the LULC map, 1999.	77
3.7 The overall classification accuracy and Kappa coefficient for the land cover map, 2002.	80
3.8 Error matrix of the LULC map, 2002.	81
3.9 The overall classification accuracy and Kappa coefficient for the land cover map, 2007.	84
3.10 Error matrix of the LULC map, 2007.	85
3.11 The commission and omission errors for the land cover map, 2007.	86
3.12 Statistical analysis for the LULC changes for 1991 and 1999.	87
3.13 Result of land use classification for 1991 and 1999 images showing the area changes of each class.	87
3.14 Statistical analysis for the LULC changes for 1991 and 2002.	88
3.15 Result of land use classification for 1991 and 2002 images showing the area changes of each class.	89



3.16	Statistical analysis for the LULC changes for 1999 and 2007.	90
3.17	Results of land use classification for 1999 and 2007 images showing the area changes of each class.	90
3.18	Statistical analysis for the LULC changes for 1991 and 2007.	92
3.19	Results of land use classification for 1991 and 2007 images showing the area changes of each class.	92
3.20	Average LST in °C for different land covers.	95
3.21	Linear regression correlation coefficients between LST in °C and NDVI by land cover types.	112
4.1	Linear regression analysis between TOA reflectance and surface reflectance retrieved from ATCOR3.	126
4.2	Linear regression analysis between LST retrieved from ATCOR3_T and NDVI method, in terms of °C for all the satellite images.	131
4.3	Comparison between LST retrieved from ATCOR3_T and NDVI method for 11 January 1991.	133
4.4	Comparison between LST retrieved from ATCOR3_T and NDVI method for 27 December 1999.	134
4.5	Comparison between LST retrieved from ATCOR3_T and NDVI method for 17 January 2002.	135
4.6	Comparison between LST retrieved from ATCOR3_T and NDVI method for 8 February 2007.	136

## LIST OF FIGURES

	PAGE
1.1 Electromagnetic spectrum.	3
2.1 The geographical feature of study area.	26
2.2 Landsat 5 TM, S1.	30
2.3 Landsat 7 ETM+, S2.	31
2.4 Landsat 7 ETM+, S3.	32
2.5 Landsat 5 TM, S4.	33
2.6 Framework applied in this research.	37
3.1 Graph of the relationship for two Landsat images, in terms of reflectance (red band).	58
3.2 Graph of the relationship for two Landsat images, in terms of reflectance (NIR band).	58
3.3 Graph of the relationship for two Landsat images, in terms of reflectance (red band).	59
3.4 Graph of the relationship for two Landsat images, in terms of reflectance (NIR band).	59
3.5 Graph of the relationship for two Landsat images, in terms of reflectance (red band).	60
3.6 Graph of the relationship for two Landsat images, in terms of reflectance (NIR band).	60
3.7 The generated NDVI map using a relative radiometric normalization for 11 January 1991 (black colour = water areas or cloud coverage).	64
3.8 The generated NDVI map using a relative radiometric normalization for 27 December 1999 (black colour = water areas or cloud coverage).	65
3.9 The generated NDVI map using a relative radiometric normalization for 17 January 2002 (black colour = water areas or cloud coverage).	66
3.10 The generated NDVI map using a relative radiometric normalization for 8 February 2007 (black colour = water areas or cloud coverage).	67

3.11	Classification map for different LULC changes over Penang Island in 1991 using Maximum Likelihood method.	70
3.12	Classification map for different LULC changes over Penang Island in 1999 using Maximum Likelihood method.	75
3.13	Classification map for different LULC changes over Penang Island in 2002 using Maximum Likelihood method.	79
3.14	Classification map for different LULC changes over Penang Island in 2007 using Maximum Likelihood method.	83
3.15	The maps of LST retrieved using ATCOR3_T for 1991, where the black colour indicated water areas or cloud coverage and is null (°C).	96
3.16	The maps of LST retrieved using ATCOR3_T for 1999, where the black colour indicated water areas or cloud coverage and is null (°C).	97
3.17	The maps of LST retrieved using ATCOR3_T for 2002, where the black colour indicated water areas or cloud coverage and is null (°C).	98
3.18	The maps of LST retrieved using ATCOR3_T for 2007, where the black colour indicated water areas or cloud coverage and is null (°C).	99
3.19	Graph of the relationship between LST and NDVI for forest area, in 1991.	101
3.20	Graph of the relationship between LST and NDVI for grassland area, in 1991.	102
3.21	Graph of the relationship between LST and NDVI for urban (highly built-up area), in 1991.	102
3.22	Graph of the relationship between LST and NDVI for urban (minimally built-up area), in 1991.	103
3.23	Graph of the relationship between LST and NDVI for barren land, in 1991.	103
3.24	Graph of the relationship between LST and NDVI for forest area, in 1999.	104
3.25	Graph of the relationship between LST and NDVI for grassland area, in 1999.	104

3.26	Graph of the relationship between LST and NDVI for urban (highly built-up area), in 1999.	105
3.27	Graph of the relationship between LST and NDVI for urban (minimally built-up area), in 1999.	105
3.28	Graph of the relationship between LST and NDVI for barren land, in 1999.	106
3.29	Graph of the relationship between LST and NDVI for forest area, in 2002.	106
3.30	Graph of the relationship between LST and NDVI for grassland area, in 2002.	107
3.31	Graph of the relationship between LST and NDVI for urban (highly built-up area), in 2002.	107
3.32	Graph of the relationship between LST and NDVI for urban (minimally built-up area), in 2002.	108
3.33	Graph of the relationship between LST and NDVI for barren land, in 2002.	108
3.34	Graph of the relationship between LST and NDVI for forest area, in 2007.	109
3.35	Graph of the relationship between LST and NDVI for grassland area, in 2007.	109
3.36	Graph of the relationship between LST and NDVI for urban (highly built-up area), in 2007.	110
3.37	Graph of the relationship between LST and NDVI for urban (minimally built-up area), in 2007.	110
3.38	Graph of the relationship between LST and NDVI for barren land, in 2007.	111
4.1	Linear regression correlation between TOA reflectance and surface reflectance for band 3 (red band) in 1991.	122
4.2	Linear regression correlation between TOA reflectance and surface reflectance for band 4 (NIR band) in 1991.	123
4.3	Linear regression correlation between TOA reflectance and surface reflectance for band 3 (red band) in 1999.	123
4.4	Linear regression correlation between TOA reflectance and surface reflectance for band 4 (NIR band) in 1999.	124

4.5	Linear regression correlation between TOA reflectance and surface reflectance for band 3 (red band) in 2002.	124
4.6	Linear regression correlation between TOA reflectance and surface reflectance for band 4 (NIR band) in 2002.	125
4.7	Linear regression correlation between TOA reflectance and surface reflectance for band 3 (red band) in 2007.	125
4.8	Linear regression correlation between TOA reflectance and surface reflectance for band 4 (NIR band) in 2007.	126
4.9	Linear regression correlation between LST retrieved from ATCOR3_T and NDVI method, in terms of °C for 1991.	129
4.10	Linear regression correlation between LST retrieved from ATCOR3_T and NDVI method, in terms of °C for 1999.	129
4.11	Linear regression correlation between LST retrieved from ATCOR3_T and NDVI method, in terms of °C for 2002.	130
4.12	Linear regression correlation between LST retrieved from ATCOR3_T and NDVI method, in terms of °C for 2007.	130

## LIST OF ABBREVIATIONS

$\mu\text{m}$	= Micrometer
ALOS-PALSAR	= Advanced Land Observation Satellite-Phased Array type L-band Synthetic Aperture Radar
ASTER	= Advanced Spaceborne Thermal Emission and Reflection Radiometer
ATCOR	= Atmospheric CORrection
ATLAS	= Advanced Thermal and Land Application Sensor
AVHRR	= Advanced Very High Resolution Radiometer
DEM	= Digital Elevation Model
DN	= Digital Number
ETM	= Enhanced Thematic Mapper
ETM+	= Enhanced Thematic Mapper Plus
GCP	= Ground Control Point
HCMM	= Heat Capacity Mapping Mission
IR	= Infrared
ITOS	= Improved TIROS Operational Satellite
Km	= Kilometer
Landsat	= Land Satellite
LIDAR	= Light Detection And Range
LOWTRAN-7	= Low Resolution Transmission
LST	= Land Surface Temperature
LULC	= Land Use/Land Cover
m	= Meter
mm	= Millimeter
MBDS	= Median-Based Directional Scaling
MSS	= MultiSpectral Scanner

MODIS	= Moderate Resolution Imaging Spectroradiometer
nm	= Nanometer
NDBaI	= Normalized Difference Bareness Index
NDBI	= Normalized Difference Built-up Index
NDVI	= Normalized Difference Vegetation Index
NDWI	= Normalized Difference Water Index
NOAA	= National Oceanic & Atmospheric Administration
OFS	= Origin Fix with Scaling
PIF	= Pseudo-Invariant Features
PIFR	= Pseudo-Invariant Feature Regression
RMSE	= Root Mean-Square Error
SAR	= Synthetic Aperture Radar
SENSAT-3	= Sensor-Atmosphere-Target
SLC	= Scan Line Correction
SMA	= Spectral Mixture Analysis
SPOT	= Satellite Pour l'Observation de la Terre
SRTM	= Shuttle Radar Topographic Mission
TM	= Thematic Mapper
TOA	= Top Of Atmosphere
UBL	= Urban Boundary Layer
UCL	= Urban Canopy Layer
UHI	= Urban Heat Island
UV	= Ultraviolet
VHRR	= Very High Resolution Radiometer

**PENILAIAN PENDERIAAN JAUH TERHADAP PERUBAHAN  
PENGUNAAN TANAH/LITUPAN TANAH DAN HUBUNGKAIT KE ATAS  
SUHU PERMUKAAN PULAU PINANG**

**ABSTRAK**

Suhu permukaan (SP) memainkan peranan yang penting dalam kajian untuk perubahan cuaca di kawasan setempat, daerah mahupun seluruh dunia. SP mengawal pembangunan sinaran haba secara anggaran antara atmosfera dan permukaan bumi. Oleh sebab itu, adalah penting bagi menilai perubahan secara mengejut dalam penggunaan tanah/litupan tanah (PTLT). Pulau Pinang, Malaysia telah mengalami perubahan yang mendadak dalam peningkatan pembangunan sejak dua dekad yang lalu disebabkan penambahan kawasan perindustrian dan perumahan. Tujuan bagi kajian ini adalah untuk mengkaji dan menilai kesan daripada SP terhadap perubahan melalui penggunaan tanah di Pulau Pinang, Malaysia. Tiga jenis teknik untuk pengkelasan terselia yang dikenali sebagai Kemungkinan Maksimum, Jarak-ke-Purata Minimum, dan Paralelepiped telah diaplikasikan untuk mengekstrak maklumat daripada imej satelit dengan menggunakan perisian komputer penderiaan jauh, iaitu PCI Geomatica 10.1. Pengkelasan bagi teknik penderiaan jauh ini membantu untuk pengujian dalam penggunaan tanah di Pulau Pinang dengan menggunakan data Landsat yang terdiri daripada pelbagai masa bagi tempoh dari 1991-2007. Kawasan latihan untuk setiap imej satelit dan tujuh kelas litupan tanah telah diperkenan bagi setiap jenis pengkelasan. Penilaian terhadap setiap jenis teknik ini telah dilakukan. Setiap peta pengkelasan telah dinilai ketepatannya dengan menggunakan data set rujukan yang mengandungi bilangan sampel yang besar, di mana ia dikumpulkan per kategori. Empat satelit imej Landsat yang ditangkap pada tahun 1991, 1999, 2002 dan 2007 telah dipilih untuk pengkelasan bagi PTLT



dengan menggunakan klasifikasi Kemungkinan Maksimum, di mana ia ditentukan daripada jalur nampak dan inframerah. Kajian ini mendapati pengkelasan menggunakan klasifikasi Kemungkinan Maksimum menghasilkan keputusan yang paling baik dan mencapai ketepatan yang tertinggi. SP dan Index Perbezaan Normalisasi Tumbuhan (IPNT) dihitung berhubung dengan perubahan dalam PTLT. Keputusan ini menunjukkan bahawa perubahan PTLT dari 1991-2007 untuk kawasan bandar (kepadatan tinggi) meningkat secara mendadak, iaitu dari 10.89 km<sup>2</sup> pada 1991 ke 65.28 km<sup>2</sup>, hampir 499.45 %. Selain itu, kawasan bandar (kepadatan rendah) juga meningkat, tetapi secara sederhana, sebanyak 57.11 %, iaitu dari 30.52 km<sup>2</sup> pada tahun 1991 ke 47.95 km<sup>2</sup> pada 2007. Sebaliknya, kawasan hutan berkurangan dengan jelas untuk tempoh 16 tahun ini, dari 126.20 km<sup>2</sup> kepada 103.64 km<sup>2</sup>, hampir 17.88 %. Sementara itu, kawasan rumput juga berkurangan sedikit dalam tempoh 16 tahun ini, kira-kira dari 84.80 km<sup>2</sup> pada 1991 kepada 83.68 km<sup>2</sup> pada 2007. Tetapi, bagi kawasan lapang, ia berkurangan secara mendadak dari tahun 1991 ke 2007, iaitu sebanyak 79.77 %. Perubahan dalam PTLT ini menunjukkan perbezaan signifikansi untuk SP di antara kawasan bandar dan luar bandar. Hubungkait yang kukuh didapati antara SP dan IPNT untuk semua kelas PTLT. Teknik penderiaan jauh yang digunakan untuk kajian ini menunjukkan teknik ini adalah efektif; ia dapat mengurangkan masa untuk analisis dalam PTPL, dan ia merupakan cara yang berguna dalam kajian ini.

**REMOTE SENSING ASSESSMENT OF LAND COVER/LAND USE  
CHANGES AND ITS RELATIONSHIP ON LAND SURFACE  
TEMPERATURE IN PENANG ISLAND**

**ABSTRACT**

Land surface temperature (LST) plays an important role in local, regional and global climate studies. LST controls the distribution of the budget for radiation heat between the atmosphere and the Earth's surface. Therefore, it is important to evaluate abrupt changes in land use/land cover (LULC). Penang Island, Malaysia has been experiencing a rapid and drastic change in urban expansion over the past two decades due to growth in industrial and residential areas. The aim of this study was to investigate and evaluate the impact of LST with respect to land-use changes in Penang Island, Malaysia. Three supervised classification techniques known as Maximum Likelihood, Minimum Distance-to-Mean and Parallelepiped were applied to the images to extract thematic information from the acquired scene by using PCI Geomatica 10.1 image processing software. These remote sensing classification techniques help to examine LULC changes in Penang Island using multi-temporal Landsat data for the period of 1991–2007. Training sites were selected within each scene and seven land cover classes were assigned to each classifier. The relative performance of each technique was evaluated. The accuracy of each classification map was assessed using a reference data set consisting of a large number of samples collected per category. Four Landsat satellite images captured in 1991, 1999, 2002 and 2007 were chosen to classify the LULC types using the Maximum Likelihood classification method, determined from visible and near-infrared bands. The study revealed that the Maximum Likelihood classifier produced superior results and achieved a high degree of accuracy. The LST and Normalised Difference Vegetation

Index (NDVI) were computed based on changes in LULC. The results showed that LULC changes from 1991-2007 for the urban area (highly built-up area) has been increased drastically, from 10.89 km<sup>2</sup> in 1991 to 65.28 km<sup>2</sup>, around 499.45 %. Besides that, the urban area (minimally built-up area) also increased moderately, about 57.11 %, from 30.52 km<sup>2</sup> in 1991 to 47.95 km<sup>2</sup> in 2007. On the contrary, forest area decreased significantly within nearly 16 years, from 126.20 km<sup>2</sup> became 103.64 km<sup>2</sup>, nearly 17.88 %. Meanwhile, the area for grassland also decreased slightly within this period, approximately 84.80 km<sup>2</sup> in 1991 to 83.68 km<sup>2</sup> in 2007. But, for barren land, the area decreased dramatically from 1991 to 2007, about 79.77 %. These changes in LULC caused at significant difference in LST between urban and rural areas. Strong correlation were observed between LST and NDVI for all LULC classes. The remote sensing technique used in this study was found to be efficient; it reduced the time for the analysis of LULC changes, and it was found to be a useful tool.

## CHAPTER 1

### INTRODUCTION OF REMOTE SENSING TECHNIQUE

#### 1.1 Introduction

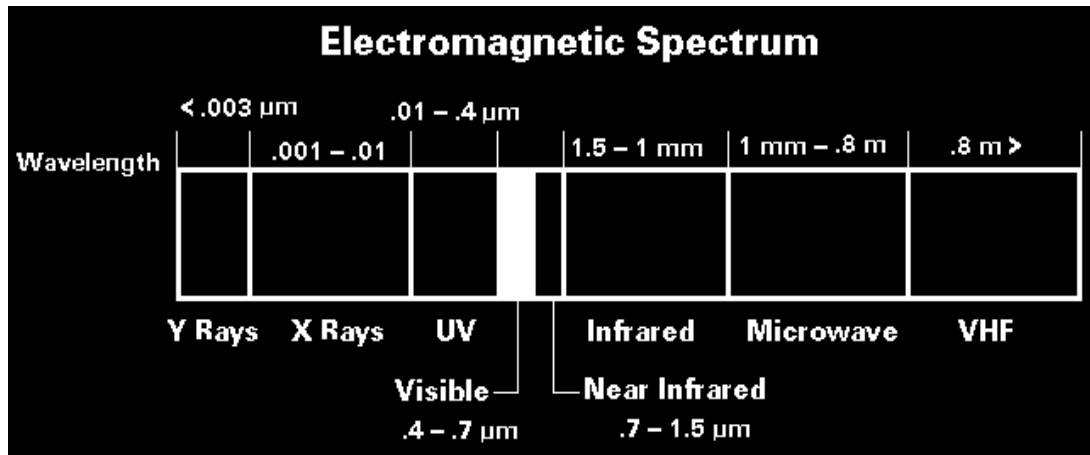
Remote sensing is defined as technique, where using a technology of science to acquire and collect information for objects, Earth's surface or phenomenon in the Earth by an observer or instrument without being in physical contact with that particular target (Siegal, 1980). Satellites and aircraft are the common instruments used to make remote sensing observation and measurement. The sensors collect information by detecting electromagnetic radiations from the targets (Lewis and Clack, 2005). This is done by measuring, recording and analyzing the electromagnetic energy, which is emitted and reflected by the objects at the Earth and atmosphere using the different types of sensors. Electromagnetic energy represents all energy that propagates in harmonic wave pattern, with the same speed of light. Electromagnetic energy includes light, heat, and radio waves.

Electromagnetic spectrum is the continuum of energy ranging from kilometers to nanometers in wavelength; propagate in the speed of light,  $3 \cdot 10^8$  m/sec. Its components range from the shorter wavelength (from gamma ray to X-ray) to the longer wavelength (including microwaves to radio waves) [Figure 1.1]. Electromagnetic radiation in different wavelengths interact differently with matter, which yield the different result of output. In remote sensing, the ultraviolet (UV), with the shortest wavelength in the spectrum has been widely used. For example, if the Earth's surface consists of minerals and rocks, they will emit visible light when irradiated with UV radiation.

The visible wavelength cover a range of approximately 0.4 (violet colour) to 0.7 nm (red colour) and it is the range of wavelength that our eyes can detect and sense. Usually sunlight is a homogenous, white colour. But, actually it consists of various wavelengths of radiation including UV, visible and infrared (IR). The visible portion of the spectrum can be easily seen when sunlight passes through a prism.

Besides that, the other portion of electromagnetic spectrum, IR is also widely applied in remote sensing. It covers the wavelengths of about 0.7  $\mu\text{m}$  to 100  $\mu\text{m}$ . IR spectrum is divided into two categories: the reflected IR (wavelength from 0.7  $\mu\text{m}$  to 3.0  $\mu\text{m}$ ) and thermal IR (wavelength from 3.0  $\mu\text{m}$  to 100  $\mu\text{m}$ ). Both of them are different in characteristic. For reflected IR, the applications used for remote sensing purposes are similar to the visible portion. While for thermal IR, the electromagnetic energy is emitted and reflected from the Earth's surface, in the form of heat. Therefore, it has different properties compared to visible and reflected IR region.

The last portion in electromagnetic spectrum is microwave, which is available in the wavelength from about 1 mm to 1 m. It has become important and widely used in remote sensing recently because it can penetrate through cloud and fog specifically the end of the spectrum. So, it is suitable for application in weather forecasting. In addition, the longer wavelengths are also being used for radio broadcasts. The shorter wavelengths in the microwave region have the same properties as thermal IR.



(Source: U.S Geological Survey EROS Data Center, 2005).

Figure 1.1. Electromagnetic spectrum.

In remote sensing, there are two types of sensors available in satellites, called passive and active sensors. A passive sensor measures the energy that is naturally radiated or reflected from an object. This energy usually comes from the sun's energy. The sensor can only record or detect the radiation energy when the naturally reflected energy is enough and available. That is one of the disadvantages for passive sensors, because the reflected energy is not available at night and the sensor cannot detect the electromagnetic energy if the sun is not illuminating the Earth. But for thermal IR, the sensor can record the information for that particular band if the total reflected energy is enough to be recorded. For active sensor, it provides its own source of energy, which is directed at the object or target and measures the reflected energy. Advantage of active sensor includes the sensor being able to detect and measure in anytime and is independent of the sun's energy. Examples of active sensors are laser fluorosensor and synthetic aperture radar (SAR).

### 1.1.1 Landsat TM/ETM+

Landsat 4 and Landsat 5 carry the sensor of Thematic Mapper (TM), are the first instrument in imaging sensor. Landsat 4 (launched on 16 July 1982) was switched off in August 1993 after the malfunction of down linking for the system. After that, Landsat 5 takes over the task of Landsat 4 through the availability of a direct data downlink system. The Landsat TM is designed with a more rapid data processing, improved data acquisition and transmission and more sophisticated sensor (Chander et al., 2009a). The TM sensor has a spatial resolution of 30 m, covering the visible, near and mid-infrared, and thermal infrared (with spatial resolution of 120 m). Landsat TM data are become more preferable as compared with Landsat Multispectral Scanner (MSS), due to the spectral, spatial, radiometric resolution over data.

The TM wavebands are as follows: Channels 1–3 cover the visible spectrum (0.45–0.52  $\mu\text{m}$ , 0.52–0.60  $\mu\text{m}$  and 0.63–0.70  $\mu\text{m}$ , representing visible blue, green and red). Channel 4 has a wavelength range of 0.75–0.90  $\mu\text{m}$  in the NIR. Channels 5 and 7 cover the mid-IR (1.55–1.75  $\mu\text{m}$  and 2.08–2.35  $\mu\text{m}$ ) while channel 6 is the thermal-IR channel (10.4–12.5  $\mu\text{m}$ ). The rather disorderly channel numbering is the result of the late addition of the 2.08–2.35  $\mu\text{m}$  band. Table 1.1 shows the properties and characteristic of Landsat.

Landsat 6 and Landsat 7 include the Enhanced Thematic Mapper (ETM) and the Enhanced Thematic Mapper Plus (ETM+) sensor, respectively. Landsat 6 was lost during the launching in October 1993. Landsat 7 replaced Landsat 6, launched on 15 April 1999 and operated successfully till mid of 2003, with the improved

version of ETM, called ETM+. The sensor measuring the upwelling radiance has the same seven bands as the TM, but with the additional 15 m resolution of panchromatic band. The spatial resolution for thermal infrared is 60 m, rather than 120 m of the TM thermal band. All the ETM+ acquisitions after May 31, 2003, have an abnormality caused by the failure of the Scan Line Correction (SLC). It offsets the motion of spacecraft to the forward and makes all the scans were adjusted parallel with each other. SLC-off images referred to the images that with data lost, while images collected prior to the SLC failure are referred to as SLC-on images.

Landsat 7 has extensively the same characteristics of operation with Landsat 4 and 5. It included a sun-synchronous orbit with an altitude of 705 km and an inclination of 98.2 °, a swath width of 185 km, and the crossing time of 10:00 at an equatorial. The orbit is the same as that of TERRA (equatorial crossing time 10:30), AQUA (equatorial crossing time 13:30) and Earth Observing-1.



Table 1.1. Landsat spectral bands and the application in remotely sensed data.

<b>Number of Band:</b>	<b>Wavelength Available (<math>\mu\text{m}</math>)</b>	<b>Description For Application In Remotely Sensed Data</b>
1	0.45-0.52 (Blue)	Band 1 useful for mapping water near coasts and also capable of differentiating soil and rock surfaces from vegetation and for detecting cultural features.
2	0.52-0.60 (Green)	Spanning the region between the blue and red chlorophyll absorption bands, this band shows the green reflectance of healthy vegetation. It is useful for differentiating between types of plants, determining the health of plants, and identifying manmade objects.
3	0.63-0.69 (Red)	The visible red band is one of the most important bands for discriminating among different kinds of vegetation. It senses in a strong chlorophyll absorption region and strong reflectance region for most soils. It has discriminated vegetation and soil. It is also useful for mapping soil type boundaries and geological formation boundaries.
4	0.77-0.90 (Near-IR)	This band is especially responsive to the amount of vegetation biomass present in a scene. It is useful for crop identification, for distinguishing between crops and soil, and for seeing the boundaries of bodies of water.
5	1.55-1.75 (Mid-IR)	This reflective-IR band is sensitive to turgidity - the amount of water in plants. Turgidity is useful in drought studies and plant vigour studies. In addition, this band can be used to discriminate between clouds, snow, and ice.
6	10.40-12.50 (Thermal-IR)	This band measures the amount of infrared radiant flux (heat) emitted from surfaces, and helps us to locate geothermal activity, classify vegetation, analyze vegetation stress, and measure soil moisture.
7	2.09-2.35 (Mid-IR)	This band is particularly helpful for discriminating among types of rock formations. Band 7 has strong water absorption region and strong reflectance region for soil and rock. Urban area, croplands, highways, bare croplands have appeared as bright tone and water body, forest have appeared as dark tone.

(Source: US. Geological Survey, 2005)

## **1.2 Urban Heat Island Effects (UHI)**

Urbanization is one form of human modifications and conversion of other types of land to uses due to the accelerated growth in human population and economy (Weng, 2001). Urbanization includes industrial, commercial and residential development promotes one of the most dramatic human-induced change of a natural ecosystem (Hung et al., 2006). Improper planning and managing the urbanization will give the direct and significant impact in local, regional and global environment. Besides that, it is the main type of land use/land cover (LULC) since few decades ago and become the major research focus (Weng and Lo, 2001).

Urban development is the main type of land cover change in the Earth (Weng and Yang, 2004). It alters the environment by deforestation and usually gives rise to dramatic change of the Earth's surface, means that all the trees and vegetations were cut down and replaced with non-evaporating and non-transpiring surfaces. Generally, the urban area has higher thermal conductivity and radiation heat budget. Therefore, by changing the vegetation area becomes impervious surfaces, such as roads, buildings, concrete, the modification of terrestrial ecosystem, the urban area tends to bring about the higher surface temperature as compared with rural area. These changes alter the solar heat radiation, surface temperature and heat storage in urban area. Heat is stored during the day and released during the night. Finally, the temperature difference between the urban and the surrounding rural area contributes to the development of an urban heat island (UHI).

There are two types of UHI which can be identified: the urban canopy layer (UCL) heat island and the urban boundary layer (UBL) heat island (Roth et al., 1989).

UCL is the layer of the urban atmosphere extending from the surface to approximately mean building height by upwardly. UBL is the layer that above the UCL, which is influenced by the underlying urban surface.

Generally, UHI studies conducted in one of two ways [Hung et al., (2006); Streutker, (2003)]: (a) measuring UHI in air temperature by using automobile transects and weather station networks and (b) measuring the UHI in the surface temperature through the airborne or satellite remote sensing. The data obtained from in-situ measurements, provided a high temporal resolution and a long time to record the data, but poor in spatial resolution. While for the thermal remote sensing, it has a higher spatial coverage or distribution but a low temporal resolution. Indeed, these data only restricted the short period for recording purpose. However, these data seldom are applied for research purposes, especially in urban climatology because it involves the enormous part to the complexity due to the interaction between atmospheric and the urban surface with the radiation within the thermal infrared band. Therefore, most of the climatology studies of UHI have been done by researchers using in-situ data, because these studies become more obvious and significant to be proved after certain periods and for a few decades.

A proper planning for effective “greening” campaigns may help to mitigate and lessening UHI effects by reducing the urban heat suffered in the urban area. One of the methods is to perform “greening” campaigns through having planted trees. Being able to plant the trees continuously can reduce the nearby air temperature through the process of transpiration (McPherson et al., 1998). Besides that, it also has advantages to modify the ecological system (Gatrell and Jensen, 2002). Furthermore,

the full information for UHI and the relationship between urban development's and the forest or vegetation in urban area can be a reference for local authorities and policy makers to determine future planning in urban design and landscape.

### **1.3 History of Thermal Infrared for Urban Climate**

From previous study done by researchers, remote sensing data in red and near-infrared (NIR) spectra have been successfully used to detect the changing of urban land covers. Satellite-derived surface temperature has been successfully used to manipulate urban climate analyses for several studies. The satellite-derived thermal data have been first analyzed by Rao, (1972) to examine the urban area. He used the Improved TIROS Operational Satellite (ITOS) to observe the surface temperature patterns for the major cities along the mid-Atlantic coast. Thermal-IR spectra available from 10.2-12.5  $\mu\text{m}$ . Carlson et al., (1977), investigated the patterns of surface temperature derived from Very High Resolution Radiometer (VHRR) in the Los Angeles region. He made comparisons between the day and night for radiant surface temperatures derived from the surface thermal (10.5-12.5  $\mu\text{m}$ ). There was a large variation between the daytime and nighttime radiant surface temperature between urban areas, such as housing area and industrial area, as compared with rural area. Besides that, Matson et al., (1978) also observed the different of radiant surface temperature between urban and surrounding rural areas by using VHRR thermal data, which was acquired at nighttime.

Price, (1979) used Heat Capacity Mapping Mission (HCMM) data (10.5-12.5  $\mu\text{m}$ ) to determine and quantify the urban surface heating in the northeastern United States. Byrne et al., (1984) came out with the result that the HCMM derived surface

radiant temperatures observed at night were linearly correlated with minimum air temperatures at the same region, such as urban and rural environments.

Kidder and Wu, (1987) investigated the St. Louis region under snow covered and snow-free conditions through Advanced Very High Resolution Radiometer (AVHRR). They utilized the multi-spectral bands, included visible (0.58-0.68  $\mu\text{m}$ ), NIR (0.72-1.1  $\mu\text{m}$ ) and thermal (3.6-3.9  $\mu\text{m}$  and 10.3-11.3  $\mu\text{m}$ ) to conduct the study. Brest, (1987) estimated the surface albedo for different season for 14 land cover types using visible (0.5-0.6  $\mu\text{m}$ ) and NIR (0.8-1.1  $\mu\text{m}$ ) Land satellite (Landsat) 1, 2 and 3 data. Meanwhile, Balling and Brazel, (1988) utilized AVHRR thermal data (10.3-11.3  $\mu\text{m}$ ) to observe the radiant surface temperature patterns in a complex urban terrain of the Phoenix, AZ region. They found that the trend of radiant surface temperature was directly correlated to the land-cover or land surface properties. The industrial regions examined 5°C greater than open land.

#### **1.4 Literature Review**

Usually, most of the research focus on UHI, based on satellite-based remote sensing, can be grouped into three main themes (Voogt and Oke, 2003): (1) to observe the spatial structure of urban thermal patterns and their relationship with the urban surface properties; (2) to study the energy balances of urban through the application of thermal remote sensing by coupling urban climate models; (3) to examine the relationship between surface UHIs and atmospheric heat islands through the combination of ground-based observations and coincident.

Past studies of urban areas due to the land surface temperature (LST) and thermal remote sensing have been conducted initially using low resolution thermal infrared imagery, such as National Oceanic & Atmospheric Administration (NOAA) AVHRR data [Gallo et al., (1993a); Kidder and Wu, (1987); Roth et al., (1989); Streutker, (2002)]; Roth et al., (1989) determined the spatial distribution for the surfaces temperatures across several cities along the west coast of North America. Through this study, it was found that for the land-use in that particular area strongly correlate with the daytime intra-urban thermal patterns. But, during nighttime, this relationship and UHI intensities was lessen. Meanwhile, my study utilized Landsat satellite images with the spatial resolution of 30 m to retrieve LST. In addition, the LULC changes were investigated in order to determine its relationship with LST.

Gallo et al., (1993a) used AVHRR data to derive radiant surface temperatures. The derivation of radiant surface temperature between urban and surrounding rural area, resulted in minimum air temperature. Besides that, the intensity of vegetation index for these particular areas was compared. Gallo et al., (1993a) highlighted the significance of the vegetation index in 37 United State cities as an obvious and important indicator in urban-rural differences in minimum air temperatures. The most important founding was the relationship between the vegetation index derived from the satellite imagery with the observed urban and rural areas. It was linearly related with each other. From all of these preliminary studies using AVHRR data, it can be concluded that it is only suitable to study the urban climate on a macro-scale due to the 1.1 km spatial resolution of AVHRR data. Therefore, it cannot provide a proper and accurate result in observing the relationships between the ground through measurements and the data derived from the satellite imagery. This means that all the

data derived from AVHRR, was not encourages to be used in data validation, as compared with the data from those measured on ground.

Beginning from the 1990s, most of urban studies shifted and focused on the study of surface temperature derivation, intra-urban temperature and the relationship between surface temperature and Earth's surface characteristic. Most of the studies conducted using medium resolution thermal infrared imagery/data, such as Landsat TM, Landsat ETM+, Advance Space borne Thermal Emission and Reflection Radiometer (ASTER), and airborne Advance Thermal and Land Application Sensor (ATLAS) data.

Carnahan and Larson, (1990), Larson and Carnahan, (1997) used Landsat TM thermal IR spectra to investigate the temperature differences between the urban and rural areas in Indianapolis. Besides that, Kim, (1992) studied the phenomenon of urban heat island in metropolitan in Washington, DC, and found the availability of moisture and soil albedo significantly in energy balance in the urban area. Nichol, (1994) attempted to utilize Landsat TM thermal data to carry out detail study by observing microclimate change for the housing estate area in Singapore. The study came out with the conclusion that the temperature derived from satellite, was highly correlated with biomass index. But, this satellite-derived data was not suitable to obtain absolute values for ambient air temperature.

More recently, Weng, (2001 and 2003) conducted studies on the surface temperature pattern and their relationship with land cover changes in urban areas for the Zhujiang Delta, China and in Guangzhou, China. Dousset and Gourmelon, (2003)

analyzed microclimate through the energy fluxes and the interaction at the urban surface of the Los Angeles and Paris metropolises based on multiple satellite sensors. Statistics of thermal IR images of Los Angeles divulge the variation of thermal patterns due to surface characteristic and atmospheric effects. But, for Paris, there was a differentiation between daytime and nighttime for heat island, and many factors of microclimates during the day influenced by surface properties. These researches help to describe the process of heat island and the effects of urbanization. Weng et al., (2004) derived the vegetation fraction from spectral mixture model, to make it becomes an alternative indicator for vegetation abundance, because traditionally normalized difference vegetation index (NDVI) has been used as the indicator of vegetation abundance to study the vegetation-LST relationship. Landsat ETM+ imagery acquired on 22 June, 2002 has been carried out to examine the relationship between these two variables. A hybrid classification procedure, combined with Maximum Likelihood and decision tree algorithms used to classify the fraction images. For spatial resolution (30-960 m), LST was having slightly stronger negative correlation with unmixed vegetation fraction than with NDVI, included all the land cover classification.

Studies have been further up using high spatial resolution (10 m) ATLAS data. Thermal IR spectra for ATLAS contributed for the wavelength in the range of 9.60-10.2  $\mu\text{m}$ , in channel 13. Most of ATLAS data applied to determine UHI effect in several cities during daytime and nighttime. Satellite-derived data showed the obvious and significant view for UHI effect over these cities by the accurately UHI patterns [Lo et al., (1997); Quattrochi et al., (2000); Quattrochi and Ridd, (1994)].



Few studies focused on the quantitative description and analysis of LST and UHIs, which was related with LULC characteristic, included biophysical variables. Gallo et al., (1993a) appraised the radiant surface temperature, vegetation index derived from satellite data and minimum air temperature in Seattle, Washington during the period of 28 June-4 July 1991. NDVI value and satellite derived radiant surface temperature demonstrate the inverse relationship in this region. Urban areas exhibit low values of NDVI, relatively high values of radiant surface temperature. But for rural areas exhibit the inverse relationship between the same variables. Both NDVI and radiant surface temperature were obviously related to minimum air temperature.

Gallo et al., (1993b) further investigated the relationship between NDVI, radiant surface temperature, and minimum air temperature for 37 cities and the nearby rural area. The satellite-derived NDVI data was linearly correlated with the in-situ minimum temperature in both urban and rural areas. Both of the urban and rural areas consisted of variety of land surface environments. The results were improved for both the variables when the elevation was taking into consideration. Furthermore, the biweekly or monthly data gave higher accuracy result as compared with daily result.

Gluch et al., (2006) assessed the overall urban thermal patterns through land cover response for Salt Lake City, Utah. In order to understand microclimate, the study carried out in the community level and the regional or valley wide level, using both airborne ATLAS and Landsat TM data. Airborne ATLAS with a high spatial resolution (10 m), are used for both land cover detection and thermal analysis at the

community level. While for the regional level, Landsat TM has been used to analysis the land cover change, but airborne ATLAS channel 13 data used for thermal analysis purpose. The result showed that the thermal response per land cover was found to be consistent at the both community and regional level, suggested the study may conduct with more coarse spatial resolution studies.

Besides that, Chen et al., (2006) studied the relationship between LULC changes and urban heat island in Pearl River Delta (PRD) in Guangdong Province, southern China, using Landsat TM and ETM+ imageries from 1990 to 2000. Results showed that UHI effect became more conspicuous in areas of rapid urbanization in PRD region through the LST patterns obtained. They found that the spatial distribution of surface temperatures has been changed from mixed patterns, where bare land, semi-bare land were experienced higher temperature, which yielded UHI. Several new indices have been developed to analyze the relationship between UHI and land cover changes, by quantitative approach between LST and several indices, including the NDVI, Normalized Difference Water Index (NDWI), Normalized Difference Bareness Index (NDBaI) and Normalized Difference Built-up Index (NDBI). It was found that NDVI, NDWI, NDBaI were negatively correlated with temperature when NDVI is limited in range, while positive correlated was shown between NDBI and temperature. A few Landsat satellite images used to determine LULC changes in PRD in Guangdong Province, southern China for 10 years period. However, in my study, few Landsat satellite images have been used in order to determine LULC changes for 16 years period.

The paper by Xian and Crane, (2005), assessed the urban growth, associated with thermal characteristic in Tampa Bay, Florida, and Las Vegas, Nevada, through the correlation of thermal IR of Landsat data with sub-pixel impervious surface. In 2002, approximately 1800 km<sup>2</sup> or 27 percent accounted for total watershed area, with sub-pixel impervious surface greater than 10%. The overall rate of increased in imperviousness is almost three-fold from 1991-2002. The study demonstrated that the values of impervious surface data may determined the pattern and urban thermal characteristic, regarding the urbanization impact with land use in urban area.

Few papers have been utilized the technique to search the relationship for urban surface biophysical descriptors and the LST. Lu and Weng, (2006) explored the thermal features and biophysical descriptors in urban area by analyzing multi-temporal ASTER image in Indianapolis, Indiana, USA. They applied linear spectral mixture analysis to derive hot-object and cold-object fractions by using five thermal infrared bands of ASTER and unmixed the nine visible, NIR, and shortwave-IR bands to calculate impervious surface, green vegetation, and soil fractions. Regression analysis was carried out to find the relationship between the computed LST from band 13 of the ASTER and the five derived variables with the spatial resolution from 15 m to 90 m. The results showed that LST was positively correlated with impervious surface, but negatively correlated with green vegetation. It also revealed that hot objects play more significant role to determine LST patterns than the cold-object.

Weng et al., (2006) developed a methodology to quantify and examine the urban landscape and LST patterns based on spectral unmixing model in Indianapolis,

Indiana. A Landsat ETM+ imagery acquired on 22 June 2002 was separately into four fractions, included vegetation, and soil, high and low albedo. A hybrid classification method was performed on the fraction images into seven land use and land cover types. Spectra mixture analysis (SMA) derived the urban surface biophysical descriptors and related to the pixel-based LST. A regression analysis used to examine the relationship between LST and impervious surface and green vegetation by study the effect of LST variations. The result revealed that the fraction images derived from SMA can provide trustworthy in measuring biophysical variables and effective in placing the development of methodology to observe the urban morphology.

More recently, Xiao and Weng, (2007) conducted study to investigate the impact of LULC changes on LST in a karst area of China. In this study, LULC changes were observed based on Landsat TM imageries from 1991-2001 in part of Guizhou Province of southern China. From the different types of LULC changes, LST and NDVI were computed. From the study, the urban areas increased dramatically, forest land increased slightly and agriculture land decreased from 1991-2001. While barren land increased from 1991-1994, and decreased from 1994-2001. The drastic changes in LULC gave the direct impact to the temperature between urban and surrounding rural areas. This temperature variation usually due to the modification of vegetation surfaces to impervious materials. It may create the warming trend in urban areas as compared with surrounding rural areas. The reforestation efforts done by government help to balance the ecosystems in rural area. In my study, I have been focused on the development of the new relationship between LST and NDVI in tropical region with respect to drastic change in LULC

changes. The strong relationship between LST and NDVI depend on the different study area and time-to-time.

Xian, (2007) evaluated the relationship between impervious surfaces and LSTs for the United States-Seattle, Washington, Tampa Bay, Florida, and Las Vegas by using both high resolution ortho-imagery and medium resolution Landsat satellite imagery. The percentage impervious surface is used as an indicator to quantify the extent and the development of urbanization in urban areas. While the LST was retrieved from a single algorithm, which was used to analyse different LULC categories in the study region. The direct effect for removal of the vegetation cover resulted with a deducing in evaporation over the urban impervious surfaces, due to the influence of surface thermal conditions. This totally yielded the UHI effects and influent on regional climatic conditions.

The paper by Hung et al., (2006) focused their study using remote sensing technique to assess the surface UHI in both temperate and tropical regions in 18 mega cities of Asian. Daytime and nighttime of Moderate Resolution Imaging Spectroradiometer (MODIS) imageries, which were least cloud acquired between 2001 and 2003 to create LST maps. The patterns of UHIs for each city were analyzed over seasonal variations. A Gaussian approximation has been performed to determine magnitude of UHIs individually for all the allocated cities. In order to divulge the relationship between UHIs with surface properties, the vegetation covers in urban areas were analyzed with surface energy fluxes derived from high resolution Landsat ETM+ data. This study gave a significant view for UHI impact in Asian mega cities and the result obtained can be used to conduct the further study through the high

spatial resolution of thermal data with LST retrieval and meso-scale modeling, and investigate the direct impacts of urbanization in local region in Asian.

From the previous study done by researchers for retrieving LST was done using split-window algorithm [Becker and Li, (1990); Jiang and Li, (2008)]. However, in my study, I used ATCOR3\_T to retrieve LST using multi-temporal satellite images. Normally, ATCOR3\_T are widely applied in Europe, by the creator, Dr R. Richter. ATCOR3\_T was tested in the tropical region in order to retrieve LST value for all the satellite images.

### **1.5 Problem Statement**

Usually, through in-situ measurement to assess LULC changes and evaluate its impact on LST for different land cover types is arduous. This is due to the time-consuming, constraint laborious, and difficulties in data processing. In addition, the availability of the historical data also restricted for certain period. Besides that, in-situ measurement can be done only for point measurement; therefore it is only restricted to study for small study area. Thus, it is difficult for assessment of LULC changes in desired study area. However, this method cannot exactly and accurately differentiate the changing of every single pixel for all the land cover types. Furthermore, the free download satellite data provided by MODIS and AVHRR to analysis LULC changes is only available and suitable to detect LULC changes for larger coverage area caused by the lower resolution of the satellite images. Therefore, this research proposed a remote sensing technique to assess LULC changes using Landsat satellite images with high spatial resolution (30 m), which is suitable for image classification in Penang Island. In addition, it is very difficult to acquire cloud-

free satellite images for long duration in Penang Island in order to assess the LULC changes. There are not many studies focused on LULC in Penang Island, especially using multi-temporal satellite images for long period.

Consequently, in-situ measurements for LST are difficult to monitor solely, and very time-consuming. Satellite measurement can provide quantitatively data with high spatial resolution or temporal-resolution (Dousset and Gourmelon, 2003). However, studies on urban climatology are less conducted due to the complexity of interactions between microwave radiations and thermal infrared with the urban surfaces and atmosphere (Voogt and Oke, 1998). Application of satellite infrared remote sensing to estimate the surface physical properties and variables has been carried out for example by [Carlson et al., (1981); Balling and Brazel, (1988); Dousset, (1989, 1991); Roth et al., (1989); Quattrochi and Ridd, (1994); Owen et al., (1998); Weng, (2001)]. Although mono-window algorithm can be applied in this study to retrieve LST value from Landsat images, however it is required many information for atmospheric parameter from the date of satellite images acquisition. Based on the thermal radiance transfer equation, its need the parameters, such as emissivity, transmittance, and effective mean atmospheric temperature (Qin et al., 2001). In this study, I proposed ATCOR3\_T technique to retrieve LST value from Landsat satellite images since it was successfully retrieved LST in Europe country, especially by the creator, Dr. R. Richter (Richter, 1998). Meanwhile, this method was less utilized in tropical region.

In Penang Island, accelerated economic development and increased of population cause the LULC to undergone abrupt change. Urban sprawl express its

stress on the environment is being witnessed of late in Penang Island and other developing country (Kumar et al., 2009). Evaluation of urban growth is necessary in order to obtain the trend and magnitude of urban growth. Furthermore, due to lack of proper planning in land use for sustainable development, rapid urban growth has bring the problem of environment, especially in ambient air temperature and LST. Hence, there is a necessary to assess and accurately describe the environment impact caused by the rampant urban growth.

The research conducted on this study based on the satellite derived LST in regional area, Penang Island. All the desired land cover types used to classify the study area using different classification methods. Urbanization impact on LST for different land cover types are carried out. Biophysical parameter such as NDVI for all the acquired satellite images also been generated to identify for their new relationship with LST in tropical region. In addition, the relationship between LST and NDVI varies due to change in study area and from time-to-time. Besides that, many studies done by researchers to develop new relationship between LST and NDVI in other country. But, there are very less study focus on the relationship between LST and NDVI in tropical region.

## **1.6 Objectives**

There are few aims or objectives when doing this research:

1. To develop new relationship between LST and NDVI for different classes of land cover after the process of classification for all the satellite images have been used.



2. To determine LULC changes in Penang Island from 1991-2007 using different types of classifiers: Maximum Likelihood, Minimum Distance-to-Mean and Parallelepiped and its relationship with LST.
3. To map LST from 1991-2007 after the retrieval using ATCOR3\_T in order to identify its relationship with LULC changes.

### **1.7 Research Scope**

From previous study done by researchers, there is not a proper study conducted on the small study area, like Penang Island using remote sensing in order to evaluate the LULC changes through multi-temporal satellite images. In addition, the impacts of improper planning for land-use bring to the variation in vegetation index, especially in NDVI. Therefore, all of these effects may affect distribution of LST for different land cover types. In this research, the study focuses on the impacts of urbanization on the Penang Island, Malaysia. The Landsat satellite images were used to evaluate urban expansion. To study the impact of urbanization, LST has been chosen to prove Penang Island, Malaysia also influent by this problem.

Seven classes of land cover used to classify the LULC changes for the study area were: forest, grassland, urban (highly built-up area), urban (minimally built-up area), barren land, water and clouds. All the classes are appropriate to classify the area in Penang because it gives the highest accuracy after classification. Three types of supervised classifiers such as Maximum Likelihood, Minimum Distance-to-Mean and Parallelepiped were applied to the images. The LULC map produced by using the Maximum Likelihood classifier shows the highest overall accuracy and Kappa coefficient statistic used among these three supervised classifiers.

Besides that, all the Landsat imageries were normalized to the same radiometric, using the relative radiometric normalization technique, to minimize the problem of atmospheric effects. Then, NDVI was computed after undergone the atmospheric correction. A few cloud detection techniques were used in this study to mask out the area of clouds on the study area so as to minimize the problem of cloud.

LST was retrieved by using ATCOR3\_T (ATmospheric CORrection) in PCI Geomatica 10.1 image processing software. LST for each class of land cover was determined based on this retrieved LST. Finally, the relationship between LST and NDVI was developed through regression analysis.

### **1.8 Summary of the Thesis**

Overall, this research focuses on the study to evaluate and analysis LULC changes in Penang Island, Malaysia using remote sensing technique. In addition, this research also developed a new relationship between LST and NDVI. Chapter 1 gives a review on the introduction regarding this study. Besides that, this chapter discusses the introduction of UHI effects, the problem statement, the objectives, and the scope of this research.

Chapter 2 explains the data pre-processing, methodology, software, and satellite images being used for this research. Besides that, every procedure for the research was described in detail. In addition, the study area and all the applied techniques for data processing were discussed. Furthermore, it also proposed the theory related with all the methods of image classification.

Chapter 3 consists of the analysis for all the obtained results for the research. The study area for LULC changes has been evaluated and compared for every land cover types within the fixed period. The impact of urbanization in LST for every land cover types also being investigated. The relationship between the NDVI and the LST for all the land cover types was analysed through a linear regression correlation.

Chapter 4 focuses on the validation for the two retrieved parameters in this research, included top of atmosphere (TOA) reflectance and LST. TOA reflectance was validated with the surface reflectance, which was retrieved using ATCOR3 in PCI Geomatica 10.1 image processing software. While LST which was retrieved using ATCOR3\_T was also validated with the LST value, generated from NDVI method.

Chapter 5 summarized all the findings or output for this research. In addition, this chapter also proposed some new techniques or procedures to conduct new research for future work. It is important in order to improve the obtained results. Furthermore, it may serve as a new finding in the future.

## **CHAPTER 2**

### **METHODOLOGY**

#### **2.1 Introduction**

The study area, materials, software and image processing methods have been discussed in detail and significant. In this chapter, the image processing software was described, in order to analyze the remotely sensed data after process will be given. The methods and the techniques used to obtain the output for research purpose will also discussed in detail. Besides that, the estimation of emissivity from the NDVI method to retrieve LST also been discussed. In addition, both the commission and omission errors are discussed in this chapter to understand the misclassifications in this study.

#### **2.2 Study Area**

The study area, Penang Island is located in the northern part of Malaysia, within latitudes 5° 12' N to 5° 30' N and longitudes 100° 09' E to 100° 26' E (Figure 2.1). George Town, the second largest city in Malaysia and also the capital city in Penang State, is located at the eastern part of Penang Island. The area of Penang Island approximately 295 km<sup>2</sup>, it is also the most populated island in the country with an estimated population of 720,000.

Penang Island enjoys a warm equatorial climate the whole year, which is warm and sunny. The average annual temperature varies between 27°-30°C, while the average mean daily temperature of about 27°C and the mean daily maximum and minimum temperatures range between 31.4 °C and 23.5 °C respectively. However,